

Coherent magnetization rotation induced by optical modulation in ferromagnetic/antiferromagnetic exchange-coupled bilayers

Ganping Ju,* Lu Chen, and A. V. Nurmikko[†]

Department of Physics and Division of Engineering, Brown University, Providence, Rhode Island 02912

R. F. C. Farrow, R. F. Marks, M. J. Carey, and B. A. Gurney

IBM Research Division, Almaden Research Center, 650 Harry Road, San Jose, California 95120-6099

(Received 21 June 1999; revised manuscript received 19 January 2000)

We have demonstrated recently that ultrafast (~ 100 ps) coherent magnetization rotation can be induced by optical modulation of the exchange coupling in an exchange coupled bilayer (NiFe/NiO) with short laser pulses [Phys. Rev. Lett. **82**, 3705 (1999)]. In this paper, we acquire further support of the coherent magnetization model by studying the details of magnetization switching dynamics, including the dependence on the amplitude of exchange bias field. The exchange bias field is subject to large transient modulation by femtosecond pulsed laser excitation, providing the impulsive force for subsequent magnetization dynamics. Good agreement is obtained with a simple model of coherent magnetization processes based on the Landau-Lifshitz-Gilbert equations of motion. We have also measured a strong dependence of the phenomenological damping constant (α) on the exchange bias in the coupled ferromagnetic/antiferromagnetic spin system.

I. INTRODUCTION

The physics of spin dynamics and magnetization reversal processes in magnetic thin films is a contemporary subject at a fundamental level and of significant application interest to the magnetic recording industry. Data rates of over 1 Gbit/sec (corresponding to less than 1 nsec magnetization reversal time) are expected within two years for hard disk drive systems, based on current extrapolations. There have been several types of experiments probing the fundamental speed ‘‘limit’’ of the dynamic switching in magnetic materials by the application of fast, pulsed magnetic fields. In a series of recent efforts, such fields are generated by various electronic and optoelectronic means in high-speed microstripline and related high-speed microwave compatible transmission lines.^{1–4} These time-resolved studies have mainly focused on switching dynamics in the nanosecond regime, although pulse widths as short as $\tau_H \sim 0.1$ nsec have been generated in exceptional cases. An entirely different approach has been adapted by Back *et al.*⁵ who acquire an intense, ultrashort pulse magnetic field ($\tau_H \approx 2-6$ psec, up to 20 KOe) by focusing a high-energy electron beam to a few square microns on a magnetic thin film. These authors demonstrated in-plane switching of the remanent state of a CoPt multilayer with perpendicular anisotropy. It was argued that for magnetic excitation occurring on time scales much shorter than the spin-lattice relaxation time τ_{SL} [on the order of $10^{-9}-10^{-10}$ sec (Ref. 5)], the thermally activated processes are ineffective so that magnetization dynamics should simply follow the Landau-Gilbert (LIG) equation of motion. Back *et al.* speculated that the initial reversal occurs by precession of magnetization *during* the duration of the ultrashort field pulse, and the magnetization subsequently relaxes into the easy direction on a much longer time scale (~ 500 ps). Their advanced experiment is conducted in such a way, however, that direct dynamical information is very difficult to obtain;

rather, this information is deduced from the ‘‘after effect’’ switching patterns which are seen to agree with a theoretical description of the switching dynamics.^{5,6} In this paper we discuss a very different approach, where the use of ultrashort laser pulses provide real-time access to magnetization switching dynamics in the precession-limited coherent rotation regime.

The approach, reported in Ref. 7, makes use of very high-speed photomodulation of the built-in *internal* effective magnetic field that is present due to the exchange coupling within an antiferromagnetic/ferromagnetic bilayer. We thus replace a time-varying external magnetic field by a transient internal field as a consequence of photoexcitation at the antiferromagnetic/ferromagnetic (AF/FM) interface. The ‘‘instantaneous’’ optical creation of a hot electron/spin gas at or near the heterointerface breaks up the exchange coupling in the bilayer, dramatically reducing the exchange bias field. This event triggers a dynamical response in the system that, as shown below, leads to coherent rotation of the magnetization vector in the FM layer. In macroscopic terms, the photoexcitation creates an induced internal ultrashort pulse magnetic field $H_{ex}(t)$ with a sub-psec rise time, inducing changes in the magnetic energy configuration of the system through a nonequilibrium, *microscopic* backdoor, so to speak.

The model system employed by us is the exchange coupled NiFe/NiO (FM/AF) bilayer, characterized by its distinct unidirectional magnetic anisotropy,⁸ utilized in giant magnetoresistance (GMR) and magnetic tunneling junction (MTJ) sensors.⁹ The magnetic characteristics of such FM/AF systems generally display the presence of a unidirectional exchange bias field H_{ex} (which rigidly shifts the hysteresis loop) as well as an increased coercivity (H_c). If the magnetization of the FM layer is initially oriented antiparallel to an external (static) applied field H_A , the optically induced ‘‘unpinning’’ of the exchange $H_{ex}(t)$ can be especially effective in providing the driving force for ultrafast switching (rotation) of magnetization. In this paper we use time-resolved

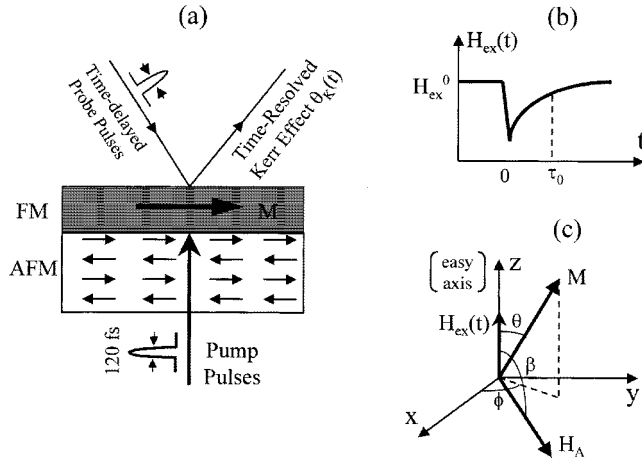


FIG. 1. (a) Schematic of the concept of optically induced “unpinning” of the exchange bias at an FM/AF interface, which triggers a coherent magnetization rotation process. (b) Definition of the coordinate system, used in the calculation of the magnetization dynamics; (c) Schematic of the temporal envelope of the time varying effective exchange bias field $H_{EX}(t)$.

techniques to learn more about the dynamics of the processes, with the magnitude H_{exch} as a variable.

II. EXPERIMENTAL RESULTS

The samples used in this study were polycrystalline NiFe/NiO bilayers grown by dc magnetron sputtering on glass substrates. The thickness of the permalloy ($\text{Ni}_{81}\text{Fe}_{19}$) layers varied in the range of 100–300 Å, while the NiO layers were approximately 400 Å thick. We studied a number of samples, with the range of exchange bias fields ranging from 15 to 100 Oe, determined by the FM layer thickness and interface microstructure. For comparison purposes, we also performed the transient experiments on single permalloy films of the same composition and thickness range, deposited directly on $\text{ZrO}_2/\text{glass}$. The optical transparency of the semi-insulating NiO at wavelengths ranging from the near infrared throughout the visible (optical gap around 3.8 eV) makes it possible to photoexcite the interface between the ferromagnet and antiferromagnet directly by directing the excitation through the NiO layer. The optical absorption depth of NiFe is less than 100 Å for the wavelength employed by us for photoexcitation.

Figure 1(a) shows the schematic of the experiment arrangement, designed for measuring optically induced transients via the longitudinal magneto-optical Kerr effect (MOKE) in a pump-probe configuration. Excitation pulses from a modelocked Ti:sapphire laser (with pulse duration of $\tau_p = 120$ fsec, photon energy of $h\nu = 1.4$ eV) were directed normal to the sample through the transparent glass substrate and the NiO layer and absorbed within the NiFe layer. Pulse-picking techniques were employed in order to reduce the laser pulse repetition rate to about 2 MHz, thus reducing average lattice heating (thermal accumulation effect) due to the poor thermal conductivity of the glass substrate. The optically induced changes in the spin/magnetization of the samples were recorded by measuring the time resolved longitudinal Kerr rotation (longitudinal) of the NiFe layer, denoted henceforth as $\theta'_K(t)$, using time delayed weak probe

pulses in the blue ($h\nu = 2.8$ eV). The choice for this probe wavelength was made in order to maximize the magneto-optical Kerr effect (MOKE) signal as well as to reject any scattered pump light. The longitudinal MOKE instrumentation employed a polarization-sensitive optical balance bridge consisting of Wallaston prism and low-noise differential photodiode pair.^{7,11,12}

In analog to the steady state case, the time-resolved MOKE signals in a pump-probe experiment include a contribution from pump-induced changes of the magnetization in the FM thin film. However, the pump-probe experiments also contain a generic contribution to $\theta'_K(t)$ from the creation of one-electron excitations by the absorption of the pump photons which leads to changes in the electron/spin distribution function and impact the optical cross section at the probe transition. Thus two distinct contributions are expected to the observed transient modulation in Kerr rotation. The first contribution is due to the modulation of spin occupancy factors in the initial and final states of the probe optical transition and the net spin polarization which tracks the relaxation of an initially nonthermal distribution of hot electron spins. Recent studies of such processes in thin FM films have given information about the dynamics of equilibration amongst the spin, electron, and lattice degrees of freedom.^{10,11} The second contribution, which is crucial to the results in this paper, reflects the proportionality of the longitudinal Kerr effect to the in-plane component of magnetization. It makes the transient experiment also sensitive to photoinduced changes in the *direction* of \mathbf{M} , e.g., due to coherent magnetization rotation.⁷

Two types of time-resolved MOKE measurement were performed in our experiments: (i) complete transient Kerr hysteresis loops were measured by sweeping the external magnetic field \mathbf{H}_A along either the easy or hard axis while recording the signal $\theta'_K(t_0)$ at a given fixed temporal delay t_0 relative to the pump and probe pulses. The transient Kerr hysteresis loops provide a measure of the external magnetic field dependence of the photoinduced transient modulation of magnetization at a given time delay. (ii) the transient Kerr signal $\theta'_K(t)$ was measured continuously as a function of the pump-probe time delay in a fixed magnetic field applied along either easy or hard axis. In this case, we acquired direct time-resolved information about the time evolution of the magnetization at a given external field. Both types of measurement are complimentary to each other and, when combined, provide a comprehensive view for the dynamical description of the coherent magnetization rotation process. We have discussed the transient Kerr loops already elsewhere⁷ and focus here on the temporal dynamics within a relatively narrow but representative range of external fields where the optically induced effects are most pronounced. In rough terms, this field range lies in the vicinity of $H_A \sim H_{ex} + H_c$, where H_c is the coercive field. Simply put, the static external field is used to bias the NiFe/NiO system near the right-hand lower corner of the steady-state hysteresis loop where the abrupt modulation of H_{ex} then has a maximum impact on magnetization dynamics. In this field range, the contribution of $\mathbf{M}(t)$ to the total measured transient Kerr signals $\theta'_K(t)$ dominates over the hot spin occupancy effects.

Figure 2 shows the measured time evolution of $\theta'_K(t)$ over

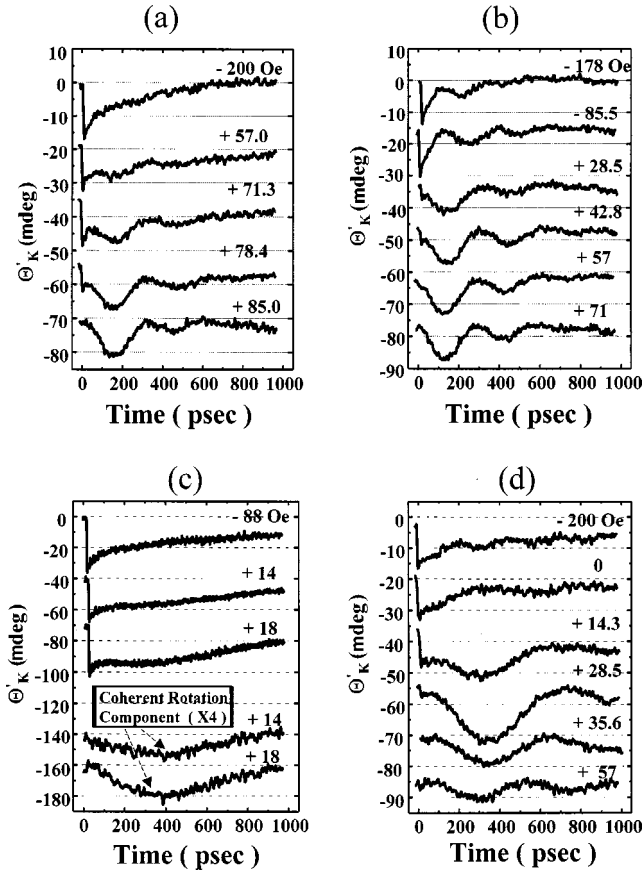


FIG. 2. (a) and (c) Time-resolved transient Kerr effect $\theta'_K(t)$ for two photoexcited NiFe/NiO bilayer samples ($H_{ex}=80$ and 15 Oe, respectively) over a range of external fields applied along the easy axis. (b) and (d) Corresponding hard axis traces.

a range of applied external field values, emphasizing the contribution due to magnetization dynamics in two photoexcited NiFe/NiO bilayer samples, with $H_{ex}=80$ and 15 Oe, respectively. These samples span a substantial range of exchange bias fields among a set of four samples studied by us, the two other bilayers having values $H_{ex}=100$ Oe (the structure subject of Ref. 7) and $H_{ex}=37$ Oe. The external bias is applied for both the easy and hard axis directions, respectively. The data exhibit the characteristic feature of damped oscillations, which emerge from the ‘hot spin’ background (one electron occupancy contribution) and dominate $\theta'_K(t)$ over a finite and specific range of magnetic fields, yielding the z components of the magnetization vector $\Delta M_z(t)/M_s$ for the easy and hard axis cases [as defined by the geometry in Figs. 1(c) and 4]. The oscillation period as well as the amplitude of oscillation is a function of both \mathbf{H}_A and \mathbf{H}_{ex} ; the first maximum can be reached in about 140 psec for the higher exchange bias sample. The companion figure (Fig. 3) shows the results of a model calculation for the two samples, described with detail in Sec. III. We defer commentary about the damping constant and its dependence on H_{ex} to this section as well. While the magnetization oscillations are pronounced over a specific range of external fields, we did make measurements over the full field range from negative to positive magnetization saturation $\pm M_s$ for the full set of four samples of differing H_{ex} . This was also helpful in explicitly measuring the hot spin occupancy factor contribution to

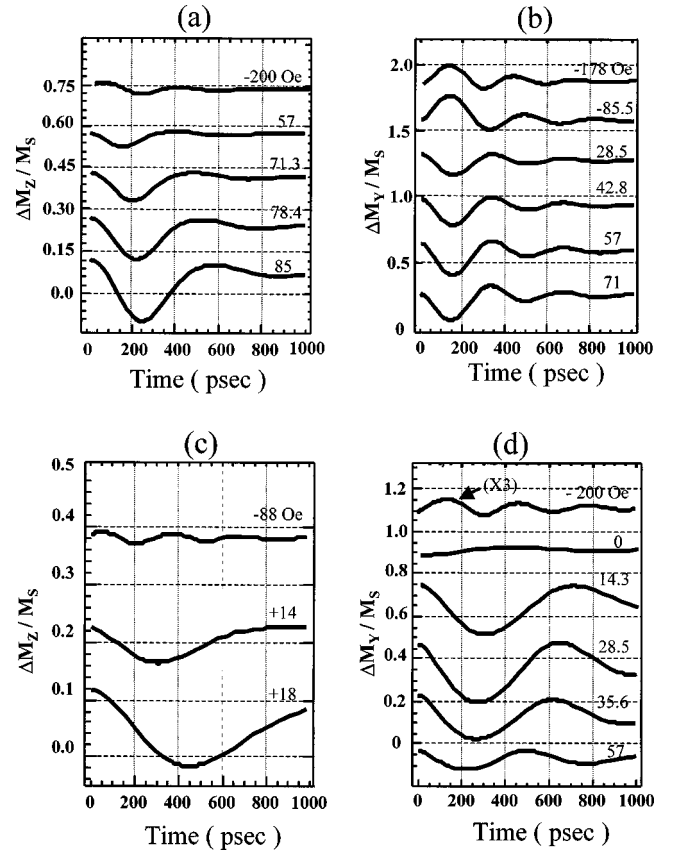


FIG. 3. Results of calculations for the two samples in Fig. 2 from the dynamical Landau-Lifshitz-Gilbert equations for applied fields along the easy axis, (a) and (c), and along the hard axis, (b) and (d). The parameter values used are modulation depth $m=0.6$, recovery time $\tau_0 \sim 100$ psec, and the damping constant $\alpha \sim 0.04$ and 0.02 , respectively.

$\theta'_K(t)$ mentioned above. For example, in full negative saturation where optically induced magnetization rotation/switching is not possible, the $\theta'_K(t)$ time traces show a very short <1 psec initial hot spin transient and a decay up to several hundred psec, as already shown in Ref. 7, yielding information, e.g., about the spin-lattice relaxation. Furthermore, as this contribution is independent of the applied field to first order, it could be subtracted out to enhance the visibility of small amplitude oscillations such as for the easy axis case of Fig. 2(c).

In the limit of full saturation, the data of Fig. 2 is very similar to that obtained on NiFe thin-film control samples, forming the basis of analyzing spin relaxation processes within a simplified three temperature model.^{10,11} Qualitatively, we note that in the easy axis configuration there is large energy barrier to be overcome before magnetization can rotate towards a well-defined second energy minimum (the two minima directed either parallel or antiparallel to H_A). On the other hand, for the hard axis configuration no such energy barrier needs to be overcome. Hence the direction of \mathbf{M} can rotate towards a favorable new energy minimum upon the modulation of the exchange coupling over a wider range of field, as discussed below. It is also worthwhile to note the larger amplitude of the contribution by coherent magnetization rotation to $\theta'_K(t)$ when the external field is applied along the hard axis (vs the easy axis). This is

especially evident in Fig. 2 for the sample with a smaller exchange bias field (15 Oe). Consistent results have been measured in another sample with relative small exchange bias ($H_{\text{ex}}=37$ Oe). In the spirit of the LLG equations applied next, these observations are consistent with the idea that the magnetization vector can be subject to more effective precessional switching by a torque applied by a pulsed field oriented at a large angle (preferably perpendicular) to the initial direction of \mathbf{M} .⁵

An additional consistency check concerning our basic premise about photoinduced transient magnetization rotation, launched by exchange bias modulation in the NiFe/NiO bilayers, was provided by two types of reference samples. First of these was a NiFe/NiO bilayer piece from the same wafer, whose exchange bias had been intentionally quenched prior to the experiment by thermal annealing. The second reference sample was a 100-Å-thick NiFe single epitaxial layer. In neither type of reference sample did we observe the distinct oscillatory time-dependent features of Fig. 2.

III. THEORETICAL CONCEPTS AND MODEL

A. Energetic considerations

One physically intuitive viewpoint about the magnetization switching induced by the optical modulation of the exchange coupling, or “unpinning” the exchange bias, can be developed from a simple energetic argument when considering the total energy of the exchange coupled bilayer system.¹⁴ As detailed elsewhere,⁷ the total energy includes three contributions. The first of these is the unidirectional anisotropy energy due to the exchange coupling across the FM/AF interface, while the second is due to the combined uniaxial bulk magnetocrystalline anisotropy K_u and the uniaxial interfacial anisotropy K_I of the FM layer. The third contribution is from the Zeeman energy. The magnetization state of the exchange coupled FM layer is determined by the energy-minimum configuration of the total energy, which is a function of the magnetization direction, applied field, uniaxial anisotropy, as well as the exchange bias.

In the transient experiments conducted here, the pump laser pulses create a nonequilibrium condition across the FM/AF interface, which modulates the exchange coupling between the ferromagnetic and antiferromagnetic spins. As noted, the process is equivalent to generating a time-varying exchange bias field $H_{\text{ex}}(t)$, sketched schematically in Fig. 1(b), whose temporal details determined by the relevant spin relaxation processes. Two special cases are particularly illustrative. Case 1: The external field is applied antiparallel to the exchange bias but with an amplitude smaller than H_{ex} such that the initial magnetization is set antiparallel to the applied field [i.e., $\theta = -180^\circ$ in the sketch of Fig. 1(c)]. By modulating the exchange coupling only, the relative energy (i.e., the energy barrier) for the two stable (parallel or antiparallel) magnetization states is varied, as shown in Ref. 7 for a specific set of real sample parameters. With a sufficient (transient) decrease in H_{ex} , the state for parallel magnetization ($\theta = 0^\circ$) becomes energetically favored over the antiparallel ($\theta = 180^\circ$) configuration. The simple adiabatic energetic consideration cannot, of course, predict the actual pathway to magnetization reversal (e.g., by coherent magnetization rotation), only that the conditions are appropriate for this to com-

mence. Case 2: The external field is applied parallel to the exchange bias (so that $\mathbf{M} \parallel \mathbf{H}_A$, i.e., $\theta = 0^\circ$). This is a configuration where maintaining a parallel magnetization remains always energetically favorable, hence no magnetization switching is possible. These predictions are consistent with our experimental results, including the qualitative shape of the transient Kerr hysteresis loops.⁷ Similar argument can be also made for the hard axis case, except that now the magnetization vector can rotate towards the direction of its new in-plane energy minimum upon the modulation of the exchange coupling for all directions of the applied field due to the lack of energy barrier.

B. Landau-Lifshitz-Gilbert equations

We now refocus on the temporal details of the optically induced magnetization rotation such as shown in the data in Fig. 2. As already noted, the temporal shape of the photo-modulated exchange bias field $H_{\text{ex}}(t)$ consists of a fast initial rise time, on the scale of about 1 psec, due to the rapid unpinning of the exchange coupling by optically excited interfacial spins. Subsequently, $H_{\text{ex}}(t)$ returns to its equilibrium state, with a time constant approximately given by the spin-lattice relaxation, or spin “cooling” time [Fig. 1(b)]. Transient Kerr measurements, performed on quenched NiFe/NiO bilayers and NiFe thin films suggest that this time constant is approximately $\tau_0 \approx 100$ psec for NiFe at room temperature for our experimental conditions. If the observed magnetization modulation is due to coherent rotation of local moments defined by each AF grain, the time dependent driving term in the relevant dynamical equations of motion is provided by $H_{\text{ex}}(t)$. The energy arguments that were sketched in the preceding section imply that, given the disappearance of the barrier for magnetization reversal within $t < 1$ psec, the magnetization will be subject to its switching towards an energetically favorable new direction. For a coherent rotation process, the actual dynamics of $\mathbf{M}(t)$ are governed by the torque applied by the time-varying total effective magnetic field. Coherent (macroscopic) magnetization dynamics are most commonly approached via the LLG equations of motion, written in the usual case of a time varying externally applied, spatially uniform magnetic field as

$$\frac{(1 + \alpha^2)}{|\gamma|} \frac{d\mathbf{M}}{dt} = -(\mathbf{M} \times \mathbf{H}_T) + \left(\frac{\alpha}{M_s} \right) [\mathbf{M} \times (\mathbf{M} \times \mathbf{H}_T)]. \quad (1)$$

We apply this formalism to study the details of the oscillatory behavior of the $\theta_K^*(t)$ traces in Figs. 2(a) and (b). We insert a total effective field into the LLG equations of the form

$$\mathbf{H}_T(t) = \mathbf{H}_A + \mathbf{H}_D + \mathbf{H}_K + \mathbf{H}_{\text{EX}}(t), \quad (2)$$

where the static applied field has the components $\mathbf{H}_A = (0, H_A \sin \beta, H_A \cos \beta)$, a uniaxial anisotropy field $\mathbf{H}_K = (0, 0, H_K \cos \theta)$, and an effective demagnetization field $\mathbf{H}_D = (-4\pi M_X, 0, 0)$ due to the shape anisotropy of the FM thin film. The coordinate system is defined in Fig. 1(c), and follows that of Ref. 6. The thin film lies in y - z plane and the easy axis is taken to be along the z direction, with θ as the angle between the magnetization and easy axis, while H_A is

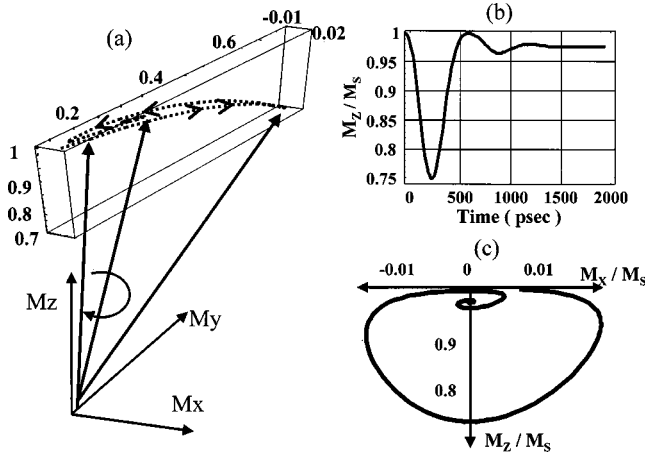


FIG. 4. Illustration of the trajectory of the magnetization vector in the typical LLG calculation. The initial direction of \mathbf{M} is directed along the z axis. \mathbf{M} is subject to a damped rotation with a large y component and a finite (out-of-plane) x component indicated schematically in (a). The transient modulation of the z component, measured by experiment, is projected out explicitly in (b), while the contour plot for the time evolution of \mathbf{M} in the x - z plane is shown in (c).

applied at an angle β with respect to the easy axis. The optically induced modulation of the exchange bias field which is entered as a time-dependent single exponential driving term with a modulation depth m [Fig. 1(b)], of the form

$$\mathbf{H}_{\text{EX}}(t) = \{0, 0, H_{\text{EX}}^0 [1 - m \cdot \exp(-t/t_0)]\}. \quad (3)$$

The rise time of $H_{\text{EX}}(t)$ is approximated as a step function and the relaxation time $\tau_0 \approx 100$ psec corresponds to the empirical spin-lattice relaxation time at the FM/AF interface extracted from our experiments, as already described.

Figure 4 shows a pictorial view of the typical LLG simulation of the dynamical magnetization rotation process. The initial direction of the magnetization vector \mathbf{M} is taken along the z axis (in the plane of the thin film). Following the photo-induced change in the exchange bias field at a time $t=0$, \mathbf{M} is subject to a damped rotation with a (potentially large) y component and a finite (out-of-plane) x component indicated schematically in Fig. 4(a). The transient modulation of the z component is projected out explicitly in the Fig. 4(b), while the contour plot for the time history of the magnetization in the x - z plane is shown in Fig. 4(c). In our experiments, the longitudinal Kerr effect geometry projects out the z component of the time-dependent magnetization vector, the data in Fig. 2 giving a measure of $\Delta M_z(t)/M_s$.

The ‘‘histograph’’ of Fig. 4 has an intuitive physical interpretation. Following the fast photoexcitation (which releases the exchange pinning field), the total effective time-varying field begins to rotate the magnetization out of the plane. The demagnetization field is initially ineffective in the absence of an out-of-plane component. However, once a finite M_x develops, a demagnetization field H_D will be generated in the $+x$ direction so that \mathbf{M} will now precess around the total effective field, including a finite H_D , towards a new equilibrium position. We emphasize that the combined presence of the demagnetizing field and the extremely short rise time (10^{-13} sec) of the effective pulse field play the domi-

nant role in determining the dynamics of $\mathbf{M}(t)$ on a picosecond time scale. The switching process is dominated by the precession (i.e., coherent rotation) triggered by the impulsive total magnetic field. On the scale of ~ 100 psec, the exchange bias field recovers and the coherent rotation is damped out through spin-wave generation and coupling to the lattice system of bilayer. We return to the subject of damping shortly.

The results of the LLG model calculations for $\Delta M_z(t)/M_s$ for the two particular NiFe/NiO samples, with $H_{\text{ex}} = 80$ Oe, and $H_{\text{ex}} = 15$ Oe ($H_C = 9$ Oe), respectively, were already shown in Fig. 3 over a specifically chosen range of external fields applied along the easy and hard axes, respectively. The calculations assumed a modulation depth $m = 0.6$. When compared with the experimental data of Fig. 2, a quite satisfactory fit is obtained for the overall damped oscillatory behavior. The oscillation period is as short as 250 psec for the higher exchange bias sample, for which the best overall fitting is obtained by choosing the recovery time for exchange coupling be equal to $\tau_0 = 100$ psec and damping constant in the LLG equations of $\alpha \sim 0.04$, with no other adjustable parameters. (We address the values of α for the other samples in the next section). In contrast, the presence of smaller amplitude oscillations with a considerably longer period (~ 700 – 800 psec) in the time traces for the sample with $H_{\text{ex}} = 15$ Oe can be readily understood by noting the smaller dynamical driving force which induces the magnetization rotation. For example, for positive applied fields from about zero to about 30 Oe along the hard axis, the amplitude and period of oscillations in the time-resolved Kerr $\theta_k^L(t)$ traces continues to increase dramatically in this sample. Maximum amplitude is reached at $H_A = +28.5$ Oe, with the magnetization rotation angle corresponding to about 45 degrees and an oscillation period of nearly 700 psec. This condition corresponds to a ‘‘critical’’ precession condition when the external field is applied along the hard axis with an amplitude H_A equal to the total effective anisotropy field, while the magnetic system is subjected to a pulse magnetic field applied perpendicular to the hard axis. When the applied field is increased further, both the amplitude and the period of the coherent magnetization rotation decrease. While such behavior is well known in studies of magnetization rotation on a slower time scale in pulsed external fields, its observation here illustrates the consistency of our interpretation that the experimental measurement of $\theta_k^L(t)$ is indeed due to the optically induced coherent magnetization rotation process.

We note that a somewhat better fitting with the LLG model to the experiment is obtained in the hard axis case, both in terms of matching the oscillation period and the damping at a given applied magnetic field. This observation might reflect the nature of the numerical approach to solving the LLG equation. The equation is usually set up for the study of magnetization reversal in such a way so as to be very sensitive to the initial conditions (the tipping angle for \mathbf{M}), especially when the total time-varying field $H_T(t)$ is applied antiparallel to the initial magnetization. In our case, we take $H_{\text{ex}}(t)$ as being single valued, and hence averaged in terms of ignoring the details of any microstructure at the exchange coupled interface. With this in mind, it is pleasing to see how the model supports at least semiquantitatively the physical picture in which the photoinduced modulation of

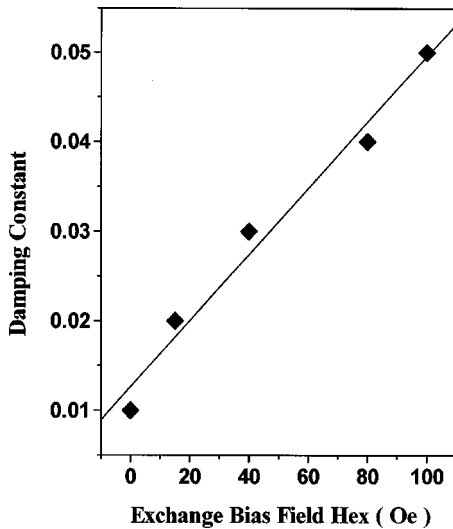


FIG. 5. The dependence of damping constant α on the magnitude of the exchange coupling.

H_{ex} provides the system the possibility for spontaneous magnetization reversal (by a simple energy argument) but where the temporal details of the magnetization dynamics are governed by driven equations of motion, with $H_{\text{ex}}(t)$ as the time-dependent “power supply.” We note that current models of the exchange bias emphasize how H_{ex} is controlled by pronounced effects due to local texture on the “mesoscopic” grain size scale.¹³ The microstructure at the NiFe/NiO interface defines a key spatial scale in the present problem, bridging between the atomic scale associated with the optically induced spin excitations and the macroscopic magnetization which is measured via $\theta_k'(t)$ in our experiments.

C. Damping of magnetization oscillations: Dependence on exchange bias

The value for the damping coefficient α , obtained from the fitting of the Landau-Lifshitz modeling of the experimental data is significantly higher for all our NiFe/NiO samples than reported for single permalloy films ($\alpha \sim 0.01$).^{2,3} Furthermore, the experiment indicates a strong dependence of α on the magnitude of the initial exchange bias. The microscopic interpretation of α is complicated by the coupled nature of the FM/AF bilayer system, which provides an extra channel for magnetic energy dissipation. From the LLG equation fits, we have extracted the phenomenological damping constant α for the set of four exchange bias samples. Figure 5 shows the dependence of α on the exchange bias field, where a nearly linear relationship seems to be apparent (a value for NiFe film is added for comparison). Recently, ferromagnetic resonance (FMR) experiments have been performed on exchange coupled ferromagnetic thin films, with the discovery that their resonance linewidth is significantly larger than that in permalloy single layer.¹⁵ Although the magnetization precession in a FMR experiment represents a very small perturbation of the system, in strong contrast to the experiments described here, the trend for an increased damping constant α is nonetheless similar. For a rough physical argument, one notes that during the coherent magnetization rotation, part of the magnetic energy of the ferro-

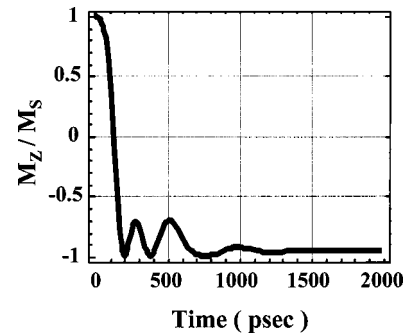


FIG. 6. Calculated results from Landau-Lifshitz-Gilbert equations for a case of $H_{\text{ex}} = 250$ Oe, predicting the case of full (irreversible) magnetization reversal by a single laser pulse.

magnetic system is dissipated through the exchange coupling between ferromagnetic and antiferromagnetic spins. The latter provides a channel of dissipation into the AF lattice system via spin-lattice relaxation. Thus the exchange coupling provides an additional means for magnetic energy dissipation when compared to a ferromagnetic single layer, where the main channel of such dissipation is confined to the spin-lattice relaxation in the ferromagnetic layer. A more detailed treatment of the damping dependence is likely to require micromagnetic modeling with the inclusion of magnon-mediated scattering processes and consideration of the microstructural details across the interface, features which are beyond the scope of the present paper but subject to future work.

IV. SUMMARY

In summary, we have explored systematically the ultrafast, optically modulated magnetization response in a ferromagnetic thin film, unidirectionally exchange coupled to an antiferromagnetic layer. The central theme of this paper has been to show that optical excitation of hot electrons and their spins in the vicinity of the FM/AF interface results in an ultrafast “unpinning” of the exchange coupling which leads to coherent magnetization rotation on a picosecond time scale. We have investigated the magnetization dynamics experimentally in some detail and shown how the data can be reasonably well matched with the dynamical Landau-Lifshitz-Gilbert equations. The dependence of the magnetization dynamics on the external magnetic field and exchange coupling strength has been studied systematically, so that a rather complete picture of the phenomenon has been acquired.

The approach described above shows that it is possible to study fast magnetization dynamics on a picosecond time scale without the need to generate external pulsed magnetic fields. Hence the photoexcitation approach provides a possibility to very high-speed control and coherent switching of magnetization through microscopic access to spins in any suitable exchange coupled system, transcending the limitations imposed by macroscopic magnetostatic energetics such as domain wall motion. Due to the noninvasive property of the optical technique, our experimental method could provide interesting approaches, for example, to the characterization of the switching dynamics of the GMR spin valve or magnetic tunneling junction sensors. Finally, the extension

of the experiments to exchange coupled magnetic systems with larger built-in unidirectional fields opens up the possibility for inducing full magnetization reversal by single laser pulse nonthermally and irreversibly. Such a tantalizing prospect is illustrated in Fig. 6 which shows the result of a LLG equation simulation for a bilayer with $H_{\text{ex}} = 250$ Oe, a value which is accessible within a number of exchange biased heterostructures. The reversal is predicted to occur in less than 100 psec and drops to ~ 10 psec for very high exchange bias/coercivity media (~ 1 KOe), according to the model. This regime may be of corollary interest to data storage applications as well. On the other hand, it raises the question whether the LLG model remains valid in such an ultrafast

(~ 1 ps) regime of magnetization reversal, or whether the microscopics of the magnetic system choose different (time-dependent) energetic pathways to accomplish the magnetization switching. Of course, the stability of such a reversed magnetization may also be subject to other energetic considerations on a longer time scale, such as those imposed by magnetic domains.

ACKNOWLEDGMENT

This research was supported by National Science Foundation Grant Nos. DMR-970159 and DMR-9871213.

*Present address: Seagate Research Center, Pittsburgh, PA 15203-2116.

†Electronic address: Arto_Nurmikko@brown.edu

¹W. D. Doyle, L. He, and P. J. Flanders, IEEE Trans. Magn. **29**, 3634 (1993); L. He, W. D. Doyle, L. Varga, H. Fujiwara, and P. J. Flanders, J. Magn. Magn. Mater. **155**, 6 (1996).

²W. K. Hiebert, A. Stankiewicz, and M. R. Freeman, Phys. Rev. Lett. **79**, 1134 (1997).

³T. J. Silva, C. S. Lee, T. M. Crawford, and C. T. Rogers, J. Appl. Phys. **85**, 7849 (1999).

⁴R. H. Koch, J. G. Deak, D. W. Abraham, P. L. Trouilloud, R. A. Altman, Yu Lu, W. J. Gallagher, R. E. Scheuerlein, K. P. Roche, and S. S. P. Parkin, Phys. Rev. Lett. **81**, 4512 (1998).

⁵C. H. Back, D. Weller, J. Heidmann, D. Mauri, D. Guarisco, E. L. Garwin, and H. C. Siegmann, Phys. Rev. Lett. **81**, 3251 (1998); C. H. Back, R. Allenspach, W. Weber, S. S. P. Parkin, D. Weller, E. L. Garwin, and H. C. Siegmann, Science **285**, 864 (1999); H. C. Siegmann, E. L. Garwin, C. Y. Prescott, J. Heidmann, D. Mauri, and D. Weller, J. Magn. Magn. Mater. **151**, L8 (1995).

⁶L. He and W. D. Doyle, J. Appl. Phys. **79**, 6489 (1996).

⁷G. Ju, A. V. Nurmikko, R. F. C. Farrow, R. F. Marks, M. J. Carey, and B. A. Gurney, Phys. Rev. Lett. **82**, 3705 (1999).

⁸W. H. Meiklejohn and C. P. Bean, Phys. Rev. **102**, 1413 (1956);

A. P. Malozemoff, Phys. Rev. B **37**, 7673 (1988); **35**, 3679 (1987); N. C. Koon, Phys. Rev. Lett. **78**, 4865 (1997).

⁹B. Dieny, V. S. Speriosu, S. S. P. Parkin, B. A. Gurney, D. R. Wilhoit, and D. Mauri, Phys. Rev. B **43**, 1297 (1991); S. Soeya, S. Tadokoro, T. Imagawa, M. Fuyama, and S. Narishige, J. Appl. Phys. **74**, 6297 (1993); H. Hamakawa, H. Hoshiya, T. Kawabe, Y. Suzuki, R. Arai, K. Nakamoto, M. Fuyama, and Y. Sugita, IEEE Trans. Magn. **32**, 149 (1996).

¹⁰E. Beaurepaire, J.-C. Merle, A. Daunois, and J.-Y. Bigot, Phys. Rev. Lett. **76**, 4250 (1996); A. Vaterlaus, T. Beutler, and F. Meier, *ibid.* **67**, 3314 (1991); J. Hohlfeld, E. Matthias, R. Knorren, and K. H. Bennemann, *ibid.* **78**, 4861 (1997).

¹¹G. Ju, A. Vertikov, A. V. Nurmikko, C. Canady, G. Xiao, R. F. C. Farrow, and A. Cebollada, Phys. Rev. B **57**, 700 (1998).

¹²G. Ju, A. V. Nurmikko, R. F. C. Farrow, R. F. Marks, M. J. Carey, and B. A. Gurney, Phys. Rev. B **58**, 11 857 (1998).

¹³K. Takano, R. H. Konama, A. E. Berkowitz, W. Cao, and G. Thomas, Phys. Rev. Lett. **79**, 1130 (1997); D. H. Han, J. G. Zhu, J. H. Judy, and J. M. Sivertsen, J. Appl. Phys. **81**, 340 (1997).

¹⁴P. A. A. van der Heijden, T. F. M. M. Maas, W. J. M. de Jonge, J. C. S. Kools, F. Roozeboom, and P. J. van der Zaag, Appl. Phys. Lett. **72**, 492 (1998); J. Appl. Phys. **83**, 7207 (1998).

¹⁵R. D. McMichael, M. D. Stiles, P. J. Chen, and W. F. Egelhoff, Jr., Phys. Rev. B **58**, 8605 (1998).